TECHNICAL MEMORANDUM

217

Impact of the ERS 1 scatterometer wind data on the ECMWF 3-D VAR Assimilation system

C. Gaffard and H. Roquet

Research Department

July 1995

European Centre for Medium-Range Weather Forecasts
Europäisches Zentrum für mittelfristige Wettervorhersage
Centre européen pour les prévisions météorologiques à moyen

1. INTRODUCTION

The ERS-1 satellite was launched on 17 July 1991 by the European Space Agency (ESA), and is carrying on board a C-band scatterometer. The ERS-1 scatterometer is a radar instrument, measuring the power backscattered towards the satellite by the earth's surface on a 500 km wide swath. It has three antennae pointing in a horizontal plane towards a direction of 45°, 90° and 135° with respect to sub-satellite track. The return signal is sampled every 25 km both along and across-track directions and can, with a good precision, be related to the 10 metre wind vector over sea (*Stoffelen and Anderson*, 1993). The major problem when retrieving wind vectors from ERS-1 scatterometer measurements is the so-called directional ambiguity, which leads most of the time to a first wind solution and a second one 180° apart, for the same backscatter measurement triplet.

ESA has implemented a ground segment, which enables numerical weather prediction centres to get ERS-1 scatterometer data in near real-time with a global coverage, through the meteorological global transmission system. These data are processed by ESA, which provides retrieved 10 metre wind vectors with ambiguity removal, as well as the instrumental parameters, necessary for the wind retrieval. The retrieval and ambiguity removal scheme, used by ESA and called CREO (*Cavanié and Lecomte*, 1987), was implemented at ECMWF, and significantly improved by *Stoffelen and Anderson* (1995), in particular from the ambiguity removal and quality control point of view. This version has been operational at ECMWF since July 1994 and is called PRESCAT.

A 2-week assimilation experiment of scatterometer wind data was performed, within the 3D-Var assimilation system currently under development at ECMWF (*Courtier et al*, 1993), for the period 6-20 December 1994. A wind speed correction was derived from a 2-year data set of collocated buoy measurements for the CMOD4 transfer function, and applied to scatterometer winds retrieved in PRESCAT. Scatterometer data are assimilated as two ambiguous wind vectors, and hence the ambiguity removal is performed implicitly within the 3D-Var analysis. The results are compared to the ones of a similar experiment, assimilating no scatterometer data. The impact of scatterometer wind data is discussed for the analysis and first-guess surface fields, in particular by comparing them with the surface observations available over sea. The short and medium range forecasts from both experiments are also examined for the 1000 hPa geopotential, and compared with the corresponding operational analyses.

2. PROCESSING AND ASSIMILATION SCHEME OF ERS-1 SCATTEROMETER DATA

2.1 Transfer function from wind to σ_0

The instrumental quantity provided by the ERS-1 scatterometer is the normalized radar cross-section, denoted σ_0, measured by each of the 3 antennae. It represents the normalized power of the signal, backscattered towards the satellite by the rough surface of the sea. It is generally related to the neutral

equivalent 10 metre wind speed and direction through an empirical transfer function (called also forward model), which enables us to compute σ_0 as a function of wind speed, relative azimuth between antenna and wind and incidence angle of the electromagnetic wave at the surface.

Before the ERS-1 launch in August 1991, a pre-launch version of the backscatter transfer function in C-band was determined and calibrated by *Long* (1985), using backscatter measurements from an airborne scatterometer and wind measurements from buoys. Not long after launch, it appeared that this transfer function was unsuitable for the ERS-1 spaceborne scatterometer, and a lot of work was carried out, in particular at ECMWF, to derive a new transfer function. *Stoffelen and Anderson* (1993) looked in detail at ERS-1 scatterometer measurements to characterize their properties and derive a suitable functional form for the transfer function, and tuned it using ECMWF 10 metre analysed winds in November 1991. The new transfer function, called CMOD4, gave very good results in terms of fitting of the measured σ_0's, and scatterometer winds retrieved using CMOD4 were in good agreement with ECMWF analysis winds, with a vector RMS difference of about 3 m/s. In that respect, scatterometer winds appeared to be of better quality than conventional wind observations at sea (ships or buoys) (*Stoffelen and Anderson*, 1993). CMOD4 has been used since 1992 by ESA to produce real-time scatterometer winds.

Since July 1994, an operational processing of ERS-1 scatterometer measurements (called PRESCAT) has been running at ECMWF, which produces systematic statistics on the quality of σ_0's and retrieved winds. This monitoring has revealed a significant underestimation of wind speeds higher than 15 m/s, when comparing scatterometer winds retrieved by PRESCAT using CMOD4, and FGAT (First-Guess at Appropriate Time) winds from the ECMWF operational model. This underestimation is illustrated in Fig 1, showing the mean and standard deviation of the difference scatterometer minus ECMWF 10 metre wind speed as a function of wind speed for nodes 5, 10 and 15, produced by the operational PRESCAT in December 1994. The total number of comparison points is here greater than 5.10^6. During the same period, pre-operational tests of the 3D-Var assimilation system were run using scatterometer wind data and, for several cases of intense storms in the Northern Hemisphere, scatterometer low bias led to an overestimate of surface pressure at the centre of the lows, in comparison with the operational analysis (differences up to 8 hPa).

A wind speed bias correction was derived for CMOD4, using a 2-year data set of collocated scatterometer and buoy wind measurements. This data set was provided by Météo-France, and consists of buoy reports received through the GTS, which are closer than 100 km in space and 3 hours in time to scatterometer measurements. This data set was screened according to the blacklisting performed by the Meteorological Operations at ECMWF for buoy observations on one hand, and using ESA's quality flags for backscatter measurements on the other hand. The resulting data set contains about 8500 collocated observations, and

a bias correction was fitted as a function of CMOD4 scatterometer wind speed, between 2 and 20 m/s, using a third degree polynomial. The coefficients of the polynomial are given in the appendix. Figure 2 is the same as Fig 1, but after the bias correction of scatterometer wind speeds. This bias correction, derived using buoy observations only, removes the scatterometer wind speed bias whatever the node number and the wind speed up to 20 m/s, in comparison with FGAT wind speeds. The overall difference standard deviation is increased by less than 0.1 m/s, mainly because of the increase of scatterometer wind speed variability for high wind speeds, and also for low wind speeds. For wind speeds higher than 20 m/s, which are taken into account in Fig 2, the bias correction was extrapolated linearly. For low wind speeds, the bias correction decreases scatterometer wind speeds, and lowers the initial CMOD4 2 m/s cut-off.

2.2 Wind retrieval and quality control

Wind retrieval and quality control are performed by PRESCAT, the operational processing chain developed and run at ECMWF, which is described and discussed in detail by *Stoffelen and Anderson* (1995). Only its main features, with stress on the quality control aspects, will be described here.

2.2.1 *Wind retrieval*

In PRESCAT, the wind retrieval is performed by minimizing the following distance from observed backscatter measurements:

$$D = \Sigma \left((\sigma obs_i)^{0.625} - (\sigma sim_i)^{0.625} \right)^2$$

where σobs_i denotes the backscatter measurement for the antenna number i, i=1, 2, 3, and σsim_i denotes the simulated value using CMOD4, which is a function of wind speed and direction. The minimization is achieved using a tabular form of the transfer function, and all the different relative minima are kept at this stage. The role of the 0.625 exponent is discussed by *Stoffelen and Anderson* (1993). This exponent is the inverse of the 1.6 exponent, which appears in the directional part of CMOD4, and allows a better isotropy of the minimization problem in the σ_0-space, avoiding wind direction trapping effects.

For the further assimilation of scatterometer winds, only two wind vector solutions are kept. The first solution $\underline{U}_1$, corresponds to the lowest minimum of D. The second one, $\underline{U}_2$, is chosen as the secondary minimum of D, which is the closest to $-\underline{U}_1$ in direction, and the residual of which is lower than three times the $\underline{U}_1$ residual. It was shown by *Stoffelen and Anderson* (1995) that the addition of a third or fourth solution did not significantly improve the quality of the retrieved wind. At the present time, scatterometer data are processed at full resolution (25 km) by PRESCAT, but are then thinned at 100 km resolution before assimilation.

2.2.2 *Quality control*

The first quality control in PRESCAT relies on the quality flags set by ESA and provided in the ERS-1 scatterometer BUFR files. The flags used are the ones related to transmission errors, antenna arcing, noise to signal ratio and land contamination. Data are also rejected, if too many individual backscatter measurements are missing for estimating the average σ_0 in the cell considered (missing packet number), or if the noise to signal ratio is larger than 10% for one of the three beams.

The other quality checks are based on additional tests performed in PRESCAT. The operational Sea Surface Temperature (SST) analysis used at ECMWF allows scatterometer measurements to be rejected, which are likely to be contaminated by sea ice. Data are rejected when the analysed SST is lower than 0°C. This temperature threshold is above the seawater freezing point, to account for possible errors in the SST analysis. Another quality control is performed after wind retrieval, based on the minimization residual for the rank 1 solution ($\underline{U}_1$). This residual represents the misfit between the empirical transfer function used, and the measured σ_0's, and contains the effects of instrumental noise and of transfer function errors. Locally, these errors can become large, for instance in the vicinity of intense and fast moving fronts, because of the effects of geophysical parameters like sea state or rain, which were not taken into account by CMOD4. *Stoffelen and Anderson* (1995) gave an average estimate of this σ_0 scatter from the cone defined by CMOD4, with a 5% constant contribution of instrumental noise, and a geophysical part dependent on wind speed and incidence angle. This geophysical noise estimate decreases with wind speed and incidence angle, leading to a maximum σ_0 scatter of about 15% at low wind speed and incidence angle. The minimization residual (called also distance to the cone) is tested for each σ_0's triplet, which is rejected if it exceeds three times the average σ_0 scatter estimate. An example of the resulting scatterometer coverage is shown in Fig 3, illustrating the overall effect of these successive quality controls. The colour scale is a function of the minimization residual, normalized by the average σ_0 scatter estimate.

A last quality control has been designed in PRESCAT, to reject scatterometer data when significant instrumental problems are present and are not accounted for quickly enough by ESA. Such problems occurred for instance during ERS-1 orbital manoeuvres or after software changes in ESA's instrumental processing chain, and are often difficult to identify when looking at retrieved winds only. This final quality control is based on the mean normalized distance to the cone (as defined above), computed over 6 hours for each node of the swath. If the mean normalized distance is found greater than 1.7 for one of the nodes, all scatterometer data are rejected from the assimilation scheme during this 6-hour interval. Figure 4 shows the monitoring of the mean distance to the cone, performed by the operational PRESCAT in March 1995. A sudden rise is detected on 22 March at 00 UT, which was found to be due to corresponding instrumental problems when ERS-1 was moved to a 35-day repeat cycle, before ERS-2 launch.

2.3 Assimilation procedure of scatterometer winds

2.3.1 *Cost function term for scatterometer observations*

As described in *Courtier et al* (1993), ECMWF's 3D-Var assimilation scheme relies on the minimization of a cost function:

$$J = J_O + J_B + J_C$$

where J_O is a quadratic term measuring the differences between the estimated control variables and the observations, J_B a quadratic term measuring the differences between the estimated control variables and the background field and J_C a penalty term expressing physical constraints on the estimated state of the atmosphere (no fast growing gravity waves).

For scatterometer data, *Stoffelen and Anderson* (1995) demonstrated that it was better to assimilate scatterometer ambiguous winds, rather than assimilating directly backscatter measurements. They showed that, because of the strong non-linearities of the transfer function from wind to backscatter measurements, it was difficult to specify adequately the error statistics in σ_0-space, to get realistic error statistics in the wind space. The two solutions $\underline{U}_1$ and $\underline{U}_2$, provided by PRESCAT (see § 2-2), are assimilated using a penalty term consisting of the following scalar function for each scatterometer wind vector pair, assuming like *Stoffelen and Anderson* (1995) that scatterometer wind errors are uncorrelated:

$$J^{scat}_o = (J_1 \, x \, J_2) / (J_1^p + J_2^p)^{1/p}$$

with:

$$J_i = (u_i - u)^2 / \Delta u^2 + (v_i - v)^2 / \Delta v^2, \; i=1, 2$$

Δu and Δv are the standard deviation of the scatterometer observation error for u and v-component of 10 metre wind, and u and v are the 10 metre wind components, related to the control variables of the variational analysis. From the comparison between scatterometer and FGAT 10 metre winds, the wind vector RMS difference is about 3.2 m/s. Assuming that both of them contain errors of the same magnitude, we obtain $\Delta\underline{U} \approx 2.3$ m/s, and hence $\Delta u = \Delta v \approx 1.6$ m/s. Slightly larger values $\Delta u = \Delta v = 2$ m/s were preferred, mainly for consistency reasons with the other surface wind observations. The empirical exponent p is set to 4. The greater p is, the more quadratic J^{scat}_o is in the vicinity of $\underline{U}_1$ or $\underline{U}_2$, given that $\underline{U}_1 \approx - \underline{U}_2$. In the 3D-Var assimilation scheme, u and v are related to the wind vector at the lower level of the analysis (currently 32 m), assuming neutral conditions in the surface boundary layer, and using the scatterometer wind speed to compute the 10 metre drag coefficient. The atmospheric stability was assumed neutral, because stability effects are generally weaker over ocean than over land, and because the CMOD4 transfer function itself relates the backscatter measurement to an equivalent neutral wind at 10 metres. To take into account the atmospheric stability, a solution would be to assimilate scatterometer observations as wind stress vectors.

2.3.2 *Implicit ambiguity removal in the 3D-Var context*

In the 3D-Var context, the directional ambiguity removal is performed implicitly during the minimization, using the two scatterometer wind solutions $\underline{U}_1$ and $\underline{U}_2$, but also using all the additional information from background field and surrounding observations, which is carried by structure functions. In that respect, one can expect that it is of better quality than the ambiguity removal performed in PRESCAT, which is based on a spatial filter (see *Stoffelen and Anderson*, 1995).

To assess the quality of the 3D-Var ambiguity removal, the scatterometer wind solution chosen by the minimization can be compared to the one selected by PRESCAT. The 3D-Var de-aliased scatterometer wind is defined as the wind solution $\underline{U}_i$, which is the closest to the analysed wind at the observation location. The wind solutions selected by PRESCAT and 3D-Var are found different for 1.5% of the cases, and this percentage is decreased to 0.7% for wind speeds higher than 4 m/s, where the scatterometer is more sensitive to wind direction. Figure 5 shows a case on 17 December 1994 south-west of the African coast, with wind speeds up to 10 m/s, where the 3D-Var (purple) has clearly corrected a PRESCAT deficiency (red).

3. IMPACT OF ERS-1 SCATTEROMETER DATA ON ANALYSIS AND FIRST-GUESS SURFACE FIELDS

The impact of scatterometer wind data on ECMWF's numerical weather prediction system is assessed by comparing two numerical experiments at spectral resolution T106 (horizontal resolution around 150 km), from 6 to 19 December 1994. This period was characterized by some intense storms in the Northern Hemisphere. The first one was run assimilating in the 3D-Var system all conventional and satellite observations used currently in the operations. In the second one, scatterometer wind data were assimilated in addition, using the CMOD4 transfer function and the wind speed bias correction described in § 2-1. Since this bias correction was tuned for wind speeds between 2 and 20 m/s only, scatterometer wind data were not assimilated if scatterometer or FGAT wind speed was higher than 20 m/s. The 3D-Var analysis was performed in both experiments using the incremental approach (*Courtier et al*, 1993), with increments computed at spectral resolution T63.

3.1 **Mean impact on analysed surface winds**

Figure 6 shows the mean wind speed difference at the lower level of the 3D-Var analysis (32 m), between the experiment assimilating scatterometer wind data (hereafter called SCATT) and the control experiment (hereafter called NOSCATT). It was computed using analyses every 6 hours, from 6 December 00h UT to 19 December 18h UT. Areas where the mean difference SCATT - NOSCATT is negative and lower than -0.25 m/s are shaded. The differences range between -1.5 and 1.5 m/s and are more significant in the Southern Hemisphere and on the western side of the tropical Indian and Pacific oceans. In the Southern

Hemisphere, SCATT winds are on average -0.25 to -0.75 m/s lower than NOSCATT winds around 50°S, where mean wind speeds are higher than 12 m/s. These features are very similar when comparing mean speed differences from SCATT and NOSCATT first-guess fields, showing that they are kept in the assimilation cycle.

The largest differences are found in western Indian and Pacific oceans, near the equator, and are probably due to stability and/or sea state effects. Figure 7 shows the mean wind vector difference SCATT - NOSCATT for the same period around 150° E. Scatterometer data tend to slow down the north-easterly winds around 10°N, and to speed up the low north-westerly winds just north of New Guinea. In these areas where wind speeds are low, swell becomes predominant in the wave spectrum (larger wave age), and the sea state can have a significant effect on the backscatter transfer function and on the 10 metre drag coefficient.

3.2 Comparison of first-guess surface fields with observations

The information brought by scatterometer wind data into the assimilation cycle can be assessed quantitatively by comparing the departures between first-guess surface fields and the surface observation which are used in the assimilation system. ERS-1 altimeter data, which are received in real-time at ECMWF, also allow wind speed comparisons with independent data.

3.2.1 *Departures from buoy wind and pressure measurements*

As a by-product, the 3D-Var assimilation system provides the values of the different J_o terms at the starting point of the minimization. They measure the departures between the background fields, provided by a 6-hour forecast of the model, and the various observation types. The results are given in Table 1 for buoy wind and pressure measurements, taken at the sea surface, in terms of RMS differences normalized by the observation error standard deviations. Most of these buoy measurements are located in the tropical Pacific ocean.

	Number of data	Exp. NOSCATT	Exp. SCATT
10 m U-comp.	1723	1.58	1.54
10 m V-comp	1723	1.29	1.27
Surface pressure	6517	1.16	1.14

Table 1: Normalized RMS differences between first-guess and buoy observations.

On average during the 2-week assimilation period these RMS differences are 3% and 2% lower for the wind u and v-components in the SCATT experiment than in the NOSCATT one. Scatterometer wind data also have a beneficial impact on surface pressure, for which departures from buoy observations are reduced by

2%. This reduction shows the consistency between the conventional buoy observations and the assimilated scatterometer wind observations, derived using CMOD4 and the wind speed bias correction described in §2.1.

3.2.2 *Comparison with scatterometer wind data*

The 10 metre winds from the first-guess at appropriate time (interpolation at the observation location and time, using model forecasts at 3, 6 and 9-hour range) are compared with the scatterometer winds from PRESCAT for the SCATT and NOSCATT experiments. This comparison can be seen as an estimate of the scatterometer information kept in a 12-hour time, as ERS-1 flies over a given geographical area at around 00 h and 12 h local time. The results for the Southern Hemisphere are presented in Fig 8, as a function of the node number in the swath, in terms of wind speed difference mean and standard deviation and in terms of wind vector RMS difference. When assimilating scatterometer wind data, the vector RMS difference is decreased by 11 cm/s in the Southern Hemisphere, and a little less in the Northern Hemisphere and in the tropics (7 cm/s and 8 cm/s respectively). The vector RMS differences increase significantly at low incidence angle (from about 3 m/s for node 19 to 4 m/s for node 1 in the Southern Hemisphere) because of the poorer directional sensitivity of the scatterometer. For this reason, scatterometer wind data from nodes 3 to 19 only are assimilated.

3.3.3 *Comparison with ERS-1 altimeter wind speeds*

The first-guess 10 metre winds are also compared with ERS-1 altimeter wind speeds, which are not assimilated into the ECMWF's numerical weather prediction system. However, these data are received in real-time and processed operationally at ECMWF together with altimeter significant wave heights, which are assimilated into the global wave model WAM. This processing includes quality control and averaging at the WAM model resolution (1.5°) (*Guillaume*, 1994). Figure 9 a) shows the corresponding bi-dimensional wind speed histogram in the Southern Hemisphere for the SCATT experiment, and Fig 9 b) its NOSCATT counterpart. Scatterometer wind data give a 10 cm/s reduction in wind speed difference standard deviation. This reduction is almost the same in the tropics (9 cm/s), and smaller in the Northern Hemisphere (4 cm/s). The bias between ERS-1 altimeter and first-guess wind speeds is also reduced from -26 cm/s to -17 cm/s with scatterometer data, corresponding to a mean decrease of 9 cm/s of the first-guess wind speeds in the Southern Hemisphere.

4. IMPACT OF ERS-1 SCATTEROMETER DATA ON FORECASTS

4.1 **Impact on short range forecasts**

The impact of ERS-1 scatterometer wind data on short range forecasts in the Southern Hemisphere is illustrated by Fig 10 a) and b). These maps show the following differences:

$$\text{RMS}\ (FC_{SCATT} - ANA_{SCATT}) - \text{RMS}\ (FC_{NOSCATT} - ANA_{SCATT})$$

computed from 6 to 19 December 1994 for 1000 hPa geopotential and for 12 and 48 hour forecasts. The green areas correspond to negative values lower than -5 m, and hence to areas where the SCATT forecasts are closer to the SCATT analyses than the NOSCATT forecasts. In yellow and orange areas, the differences are greater than 5 m. Similar plots show very little impact of scatterometer wind data in the Northern Hemisphere.

For the 12 hour forecasts, the impact of scatterometer wind data is positive or neutral almost everywhere in the Southern Hemisphere, in comparison with the SCATT analyses. The maximum impact is found north-west of New Zealand, with a 15 m reduction of the RMS. Most of the other areas of significant impact are found around 60°S. For the 48 hour forecasts, the area of positive impact north-west of New Zealand has extended and deepened, with a maximum RMS reduction of 20 m. Another significant area of positive impact is found at the same longitude, around 60°S. However, in the rest of the Southern Hemisphere, the areas of positive impact are much more scattered than for the 12 hour forecasts, and many spots of negative impact have also appeared, which counterbalance them. At 48 hour forecast range, a significant part of the beneficial impact of scatterometer wind data on the 1000 hPa geopotential seems to be lost.

4.2 Impact on medium range forecasts

The impact of scatterometer wind data on medium range forecast is assessed in the usual way, by comparing SCATT and NOSCATT forecasts with the operational analysis in different areas of the globe. Note that the operational analysis was performed at spectral resolution T213 by an optimal interpolation method, and does not use any scatterometer data. In most of the scatterometer data assimilation experiments performed so far at ECMWF or in other numerical weather prediction centres (see e.g. *Bell*, 1993) at the global scale, most of the positive impact on the forecasts was found in the Southern Hemisphere, where fewer conventional observations are available. From the 14 cases of our assimilation experiment, the impact of scatterometer wind data on 1000 hPa geopotential is found slightly positive or neutral whatever the area, with a maximum over Northern America. These comparisons are shown in Fig 11 a) and b), for Northern America and the Southern Hemisphere in terms of anomaly correlation and RMS of the 1000 hPa geopotential as a function of forecast range. This is probably due to the particular meteorological regime during this period, with storms developing in the eastern part of the northern Pacific. On the other hand, the impact in the Southern Hemisphere is hardly noticeable when comparing SCATT and NOSCATT forecasts with the operational analysis.

A particular case is shown in Figs 12 and 13 where the scatterometer wind data have brought a significant improvement to the 96 hour forecast, although the SCATT and NOSCATT analyses were rather similar. Figure 12 a) and b) shows the 1000 hPa geopotential analysis on 17 December 1994 at 12 UT, in the

SCATT and NOSCATT experiments. Two low pressure systems are present in the northern Pacific, with very similar minimum values in both cases (-249 m and -215 m in the SCATT case, -250 m and -211 m in the NOSCATT case). A scatterometer swath was present around 165°W, leading to a decrease in the surface pressure and a reduction of the cut-off between the two lows in the SCATT case. This change of structure led to a significant difference in the 96 hour forecast (Fig 13 a) and b)), in the intensity of the low located around 155°W, 45°N. The forecast minimum value is -208 m in the SCATT case, which compares much better with the operational analysis (-254 m) shown in Fig 13 c) than in the NOSCATT case (-166 m).

5. SUMMARY AND CONCLUSION

An assimilation experiment of ERS-1 scatterometer wind data was performed in ECMWF's 3D-Var system for a 2-week period from 6 to 20 December 1994. In this experiment we used a new version of the CMOD4 transfer function in which the wind speed dependency was re-tuned using a collocated data set of buoy measurements. This correction removes the former CMOD4 low bias for high wind speeds. Wind retrieval and quality controls are performed in a pre-processor called PRESCAT, and scatterometer wind data which have passed the quality criteria are assimilated in the 3D-Var system as pairs of ambiguous wind vectors with a 100 km horizontal sampling. The ambiguity removal is done implicitly during the 3D-Var analysis, using all the information from the background and the other observations.

During this assimilation experiment, the implicit ambiguity removal within 3D-Var has proved to work well, giving very similar results to the statistical scheme in PRESCAT. The results of the experiment assimilating scatterometer wind data were compared to the ones of a parallel experiment, without scatterometer wind data. When assimilating scatterometer wind data, the departures between first-guess wind fields and buoy, scatterometer or altimeter winds are decreased. The reduction of the departures from scatterometer and altimeter winds is maximum in the Southern Hemisphere.

The impact of scatterometer wind data on the short and medium range forecasts has been investigated for 1000 hPa geopotential. For short range forecasts, a significant impact is found in the Southern Hemisphere only. Taking the 3D-Var analysis using scatterometer wind data as reference, the scatterometer wind data have a clear positive impact on the 12 hour forecasts in the Southern Hemisphere, a significant part of which is lost in the 48 hour forecasts. For medium range forecasts, and taking the operational analysis as reference, the impact of scatterometer wind data is found slightly positive or neutral whatever the geographical area of the globe, with a maximum positive impact over Northern America. This feature is likely due to the particular meteorological regime during this period, with storms developing in the eastern part of the northern Pacific.

Scatterometer wind data, as other surface observations, are difficult to use in sequential assimilation schemes as optimal interpolation or 3D-Var in which the horizontal and vertical structure functions used for the background errors are predefined and do not depend on the meteorological conditions. To that respect, the 4D-Var assimilation methods are very promising (*Thépaut et al*, 1993). However, scatterometer wind data can already be beneficial for the analyses and short term forecasts, in particular in the areas where few conventional observations are available. For this reason, the assimilation of scatterometer wind data in the numerical weather prediction systems should also be beneficial for wave and ocean modelling, which are very dependent on the quality of surface wind fields.

ACKNOWLEDGEMENTS

The authors would like to thank Björn Hansen, who produced the comparisons between ERS-1 altimeter and model 10 metre wind speeds.

REFERENCES

Bell, R S, 1993: "Operational use of ERS-1 products in the meteorological office", proceedings of the second ERS-1 Symposium, Hamburg, Germany, 11-13 October 1993, pp. 195-200, ESA publication.

Cavanié, A and P Lecomte, 1987: "Study of a method to dealias winds from ERS-1 data", Final report of ESA contract No 6874/87/CP-I, vol. 1, ESA publication.

Cavanié, A and P Lecomte, 1987: "Wind retrieval and dealiasing subroutines", Final report of ESA contract No 6874/87/CP-I, vol. 2, ESA publication.

Courtier, P et al, 1993: "Variational assimilation at ECMWF", ECMWF Research Department Tech Mem 194.

Long, A, 1985: "Towards a C-band radar sea echo model for the ERS-1 scatterometer", proceedings of the third international Symposium on spectral signatures, pp. 29-34, ESA publication.

Guillaume, A, 1994: "Accuracy of the ERS-1 altimeter-derived Fast Delivery Products for wave data assimilation", ECMWF Research Department Tech Mem 198.

Hoffman, R, 1993: "A preliminary study of the impact of the C-band scatterometer wind data on global scale numerical weather prediction", J Geophys Res, 98 (C6), pp. 10233-10244.

Stoffelen, A, C Gaffard and D Anderson, 1993: "ERS-1 scatterometer data assimilation", proceedings of the second ERS-1 Symposium, Hamburg, Germany, 11-13 October 1993, pp. 191-194, ESA publication.

Stoffelen, A and D Anderson, 1993: "Characterisation of ERS-1 scatterometer measurements and wind retrieval", proceedings of the second ERS-1 Symposium, Hamburg, Germany, 11-13 October 1993, pp. 997-1001, ESA publication.

Stoffelen, A and D Anderson, 1995: "The ECMWF contribution to the characterisation, interpretation, calibration and validation of ERS-1 scatterometer backscatter measurements and winds, and their use in the Numerical Weather Prediction models", ESA contract report.

Thépaut, J-N, R Hoffman and P Courtier, 1993: "Interactions of dynamics and observations in a four-dimensional variational system", Mon Wea Rev, 121, No. 12, pp. 3393-3414.

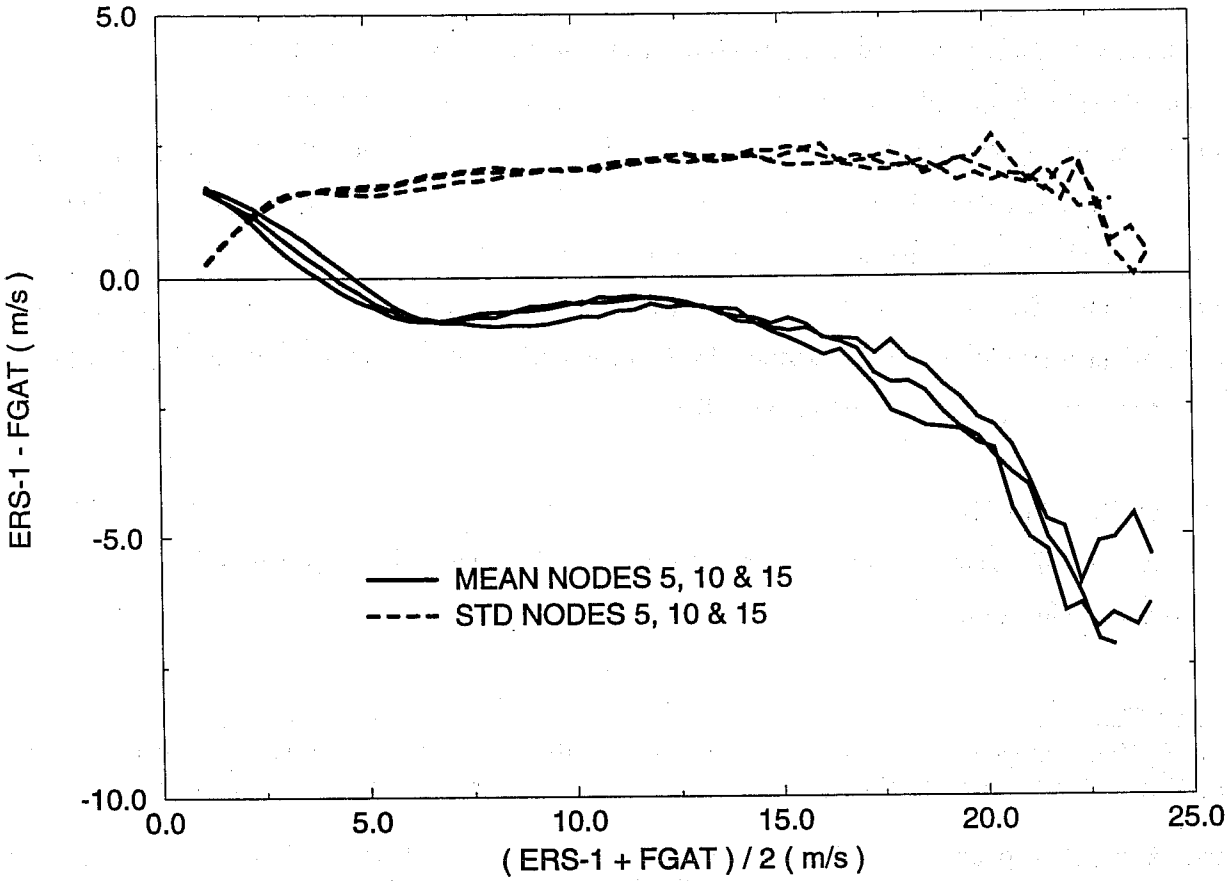

Fig 1: Mean and standard deviation of the 10 metre wind speed difference scatterometer minus FGAT (First Guess at Appropriate Time) in December 1994 as a function of wind speed for nodes number 5, 10 and 15. The scatterometer wind was retrieved using the CMOD4 transfer function.

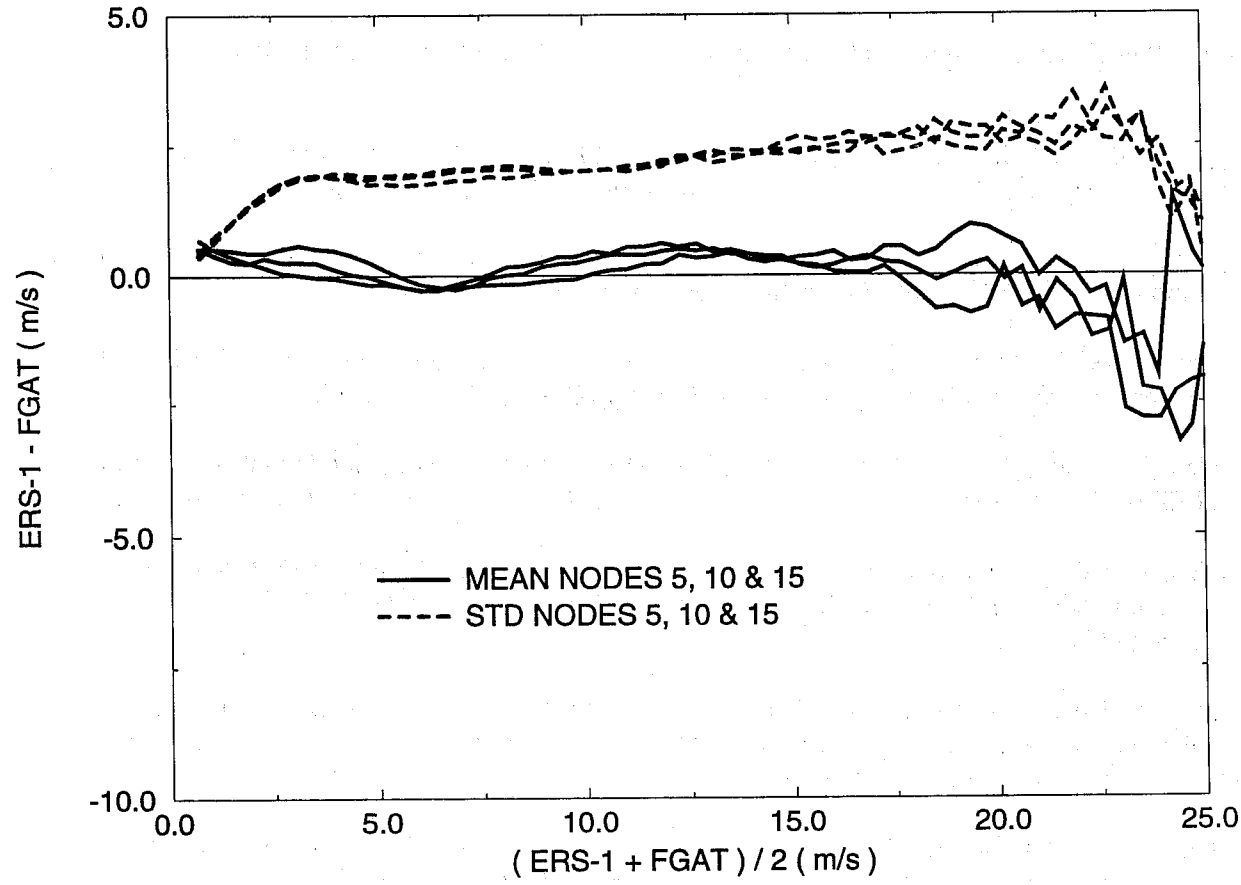

Fig 2: Same as Fig 1, but after correction of the scatterometer wind speed bias.

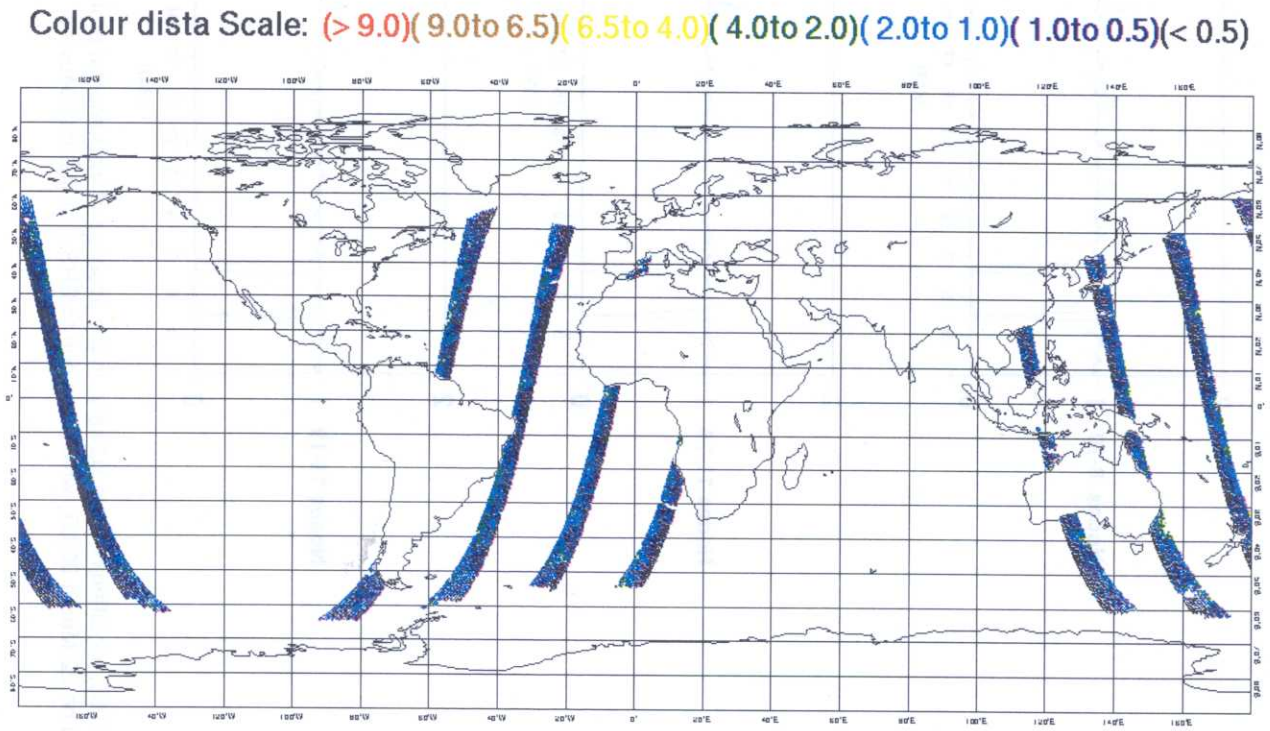

Fig 3: Coverage map of scatterometer wind data on 17 December 1994 between 09 UT and 15 UT, which have passed the PRESCAT quality controls. The colours are a function of the normalized minimization residual.

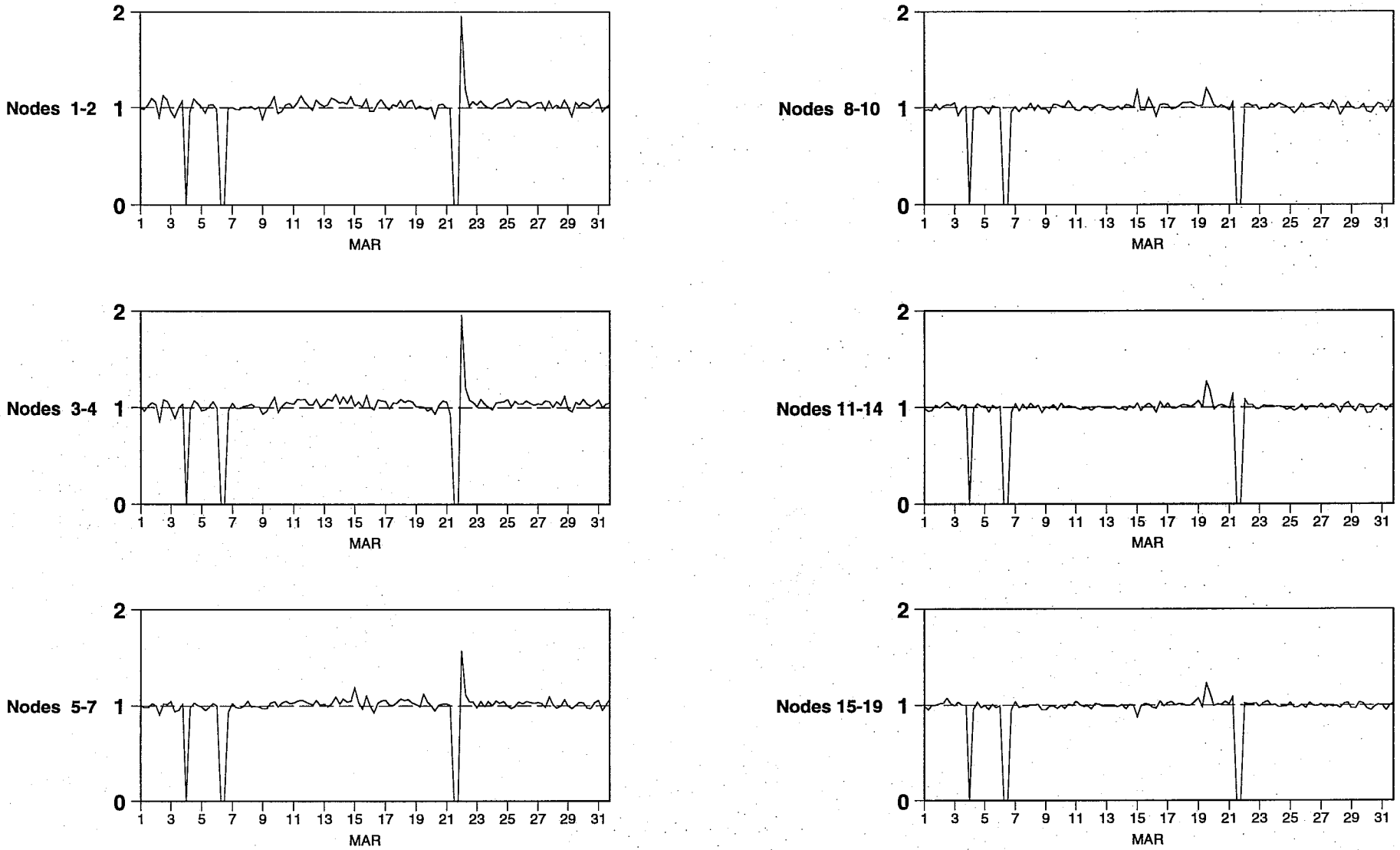

Fig 4: Monitoring of the mean normalized distance of σ0's to the cone, in March 1995, for different node subsets. In the absence of instrumental problems, this distance (solid line) should be close to 1, whatever the node number. A problem was detected on 22 March 00 UT, which was due to ERS-1 orbital manoeuvres.

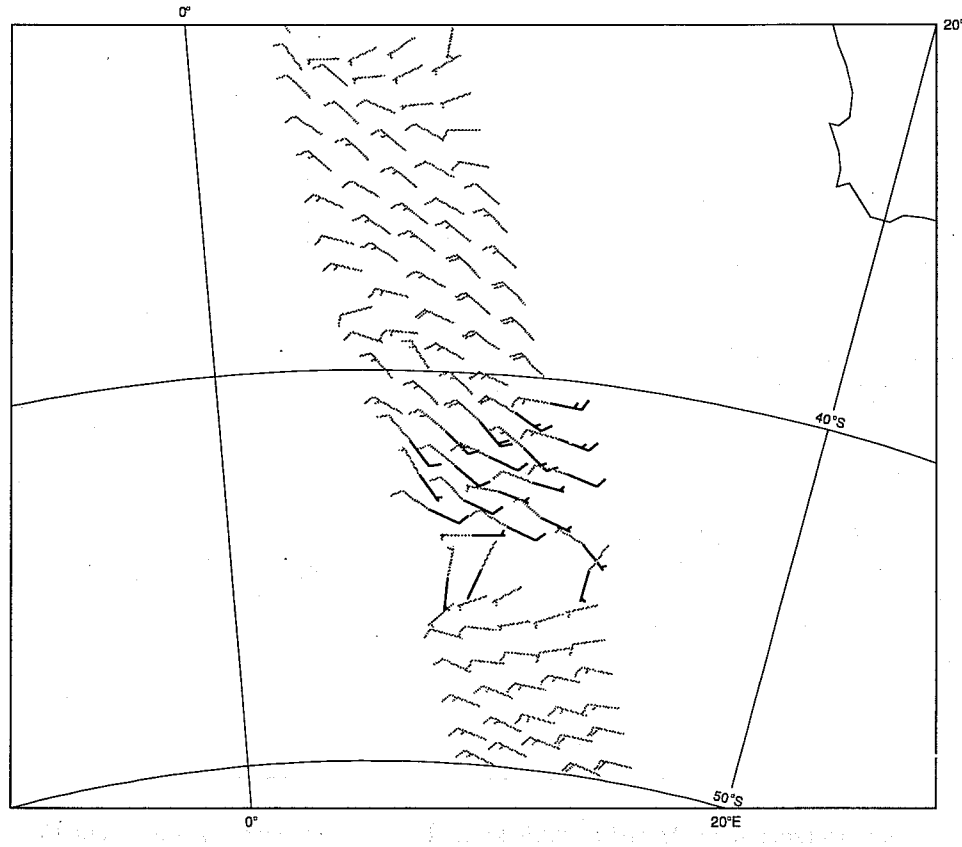

Fig 5: Comparison of scatterometer winds dealiased by PRESCAT (black wind flags) and by the 3D-Var assimilation system (grey wind flags), on 17 December 1994 at 00 UT. PRESCAT solutions are visible only when they differ from the 3D-Var ones.

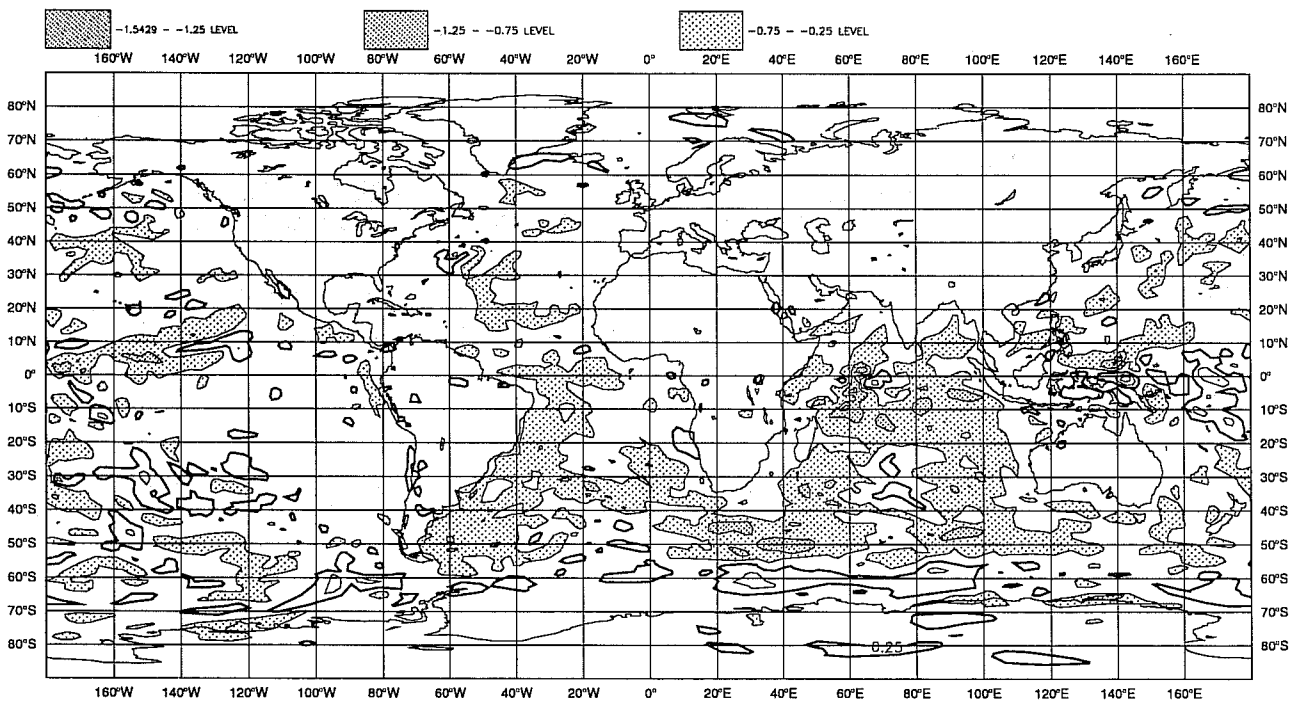

Fig 6: Mean wind speed difference at the lowest analysis level (32 m), between analyses with and without scatterometer wind data, computed over the period 6-19 December 1994. The reference contour level is 0.25 m/s, the contour interval is 0.5 m/s and the shaded areas correspond to mean differences SCATT - NOSCATT lower than -0.25 m/s.

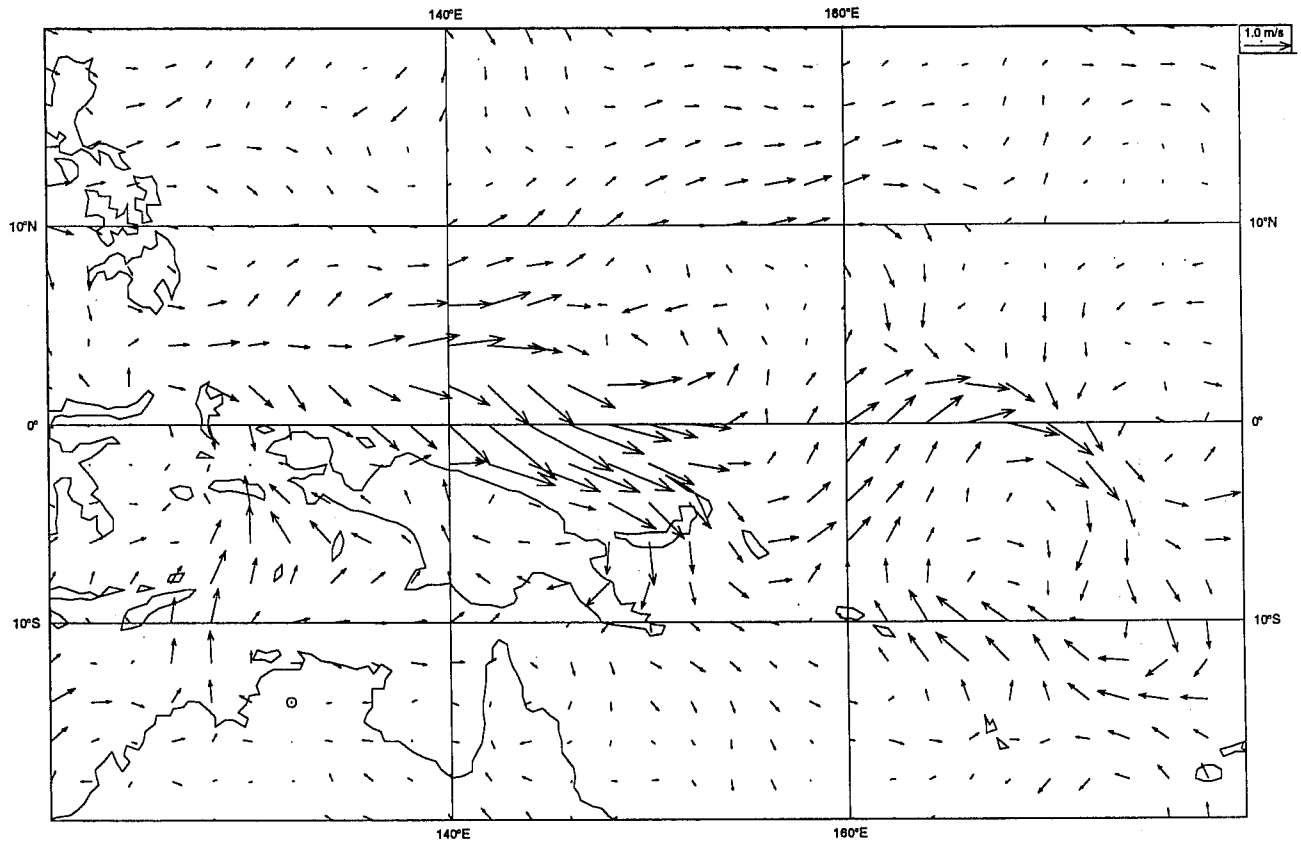

Fig 7: Mean wind vector difference at the lowest analysis level (32 m) between analyses with and without scatterometer wind data computed over the period 6-19 December 1994. The maximum wind difference is 2 m/s.

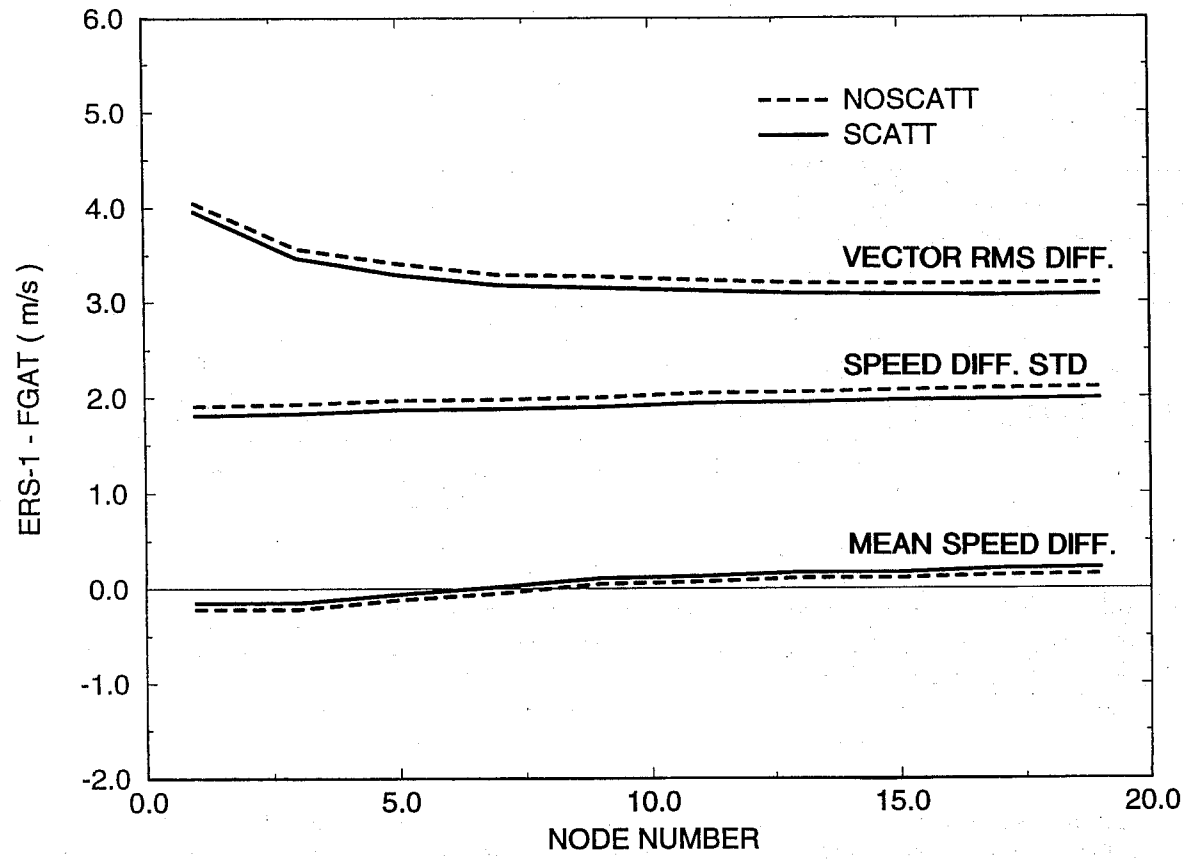

Fig 8: Departure statistics between scatterometer and FGAT winds in the Southern Hemisphere for the SCATT and NOSCATT experiments. They are computed as a function of node number from 1 (low incidence angle) to 19 (high incidence angle).

a)

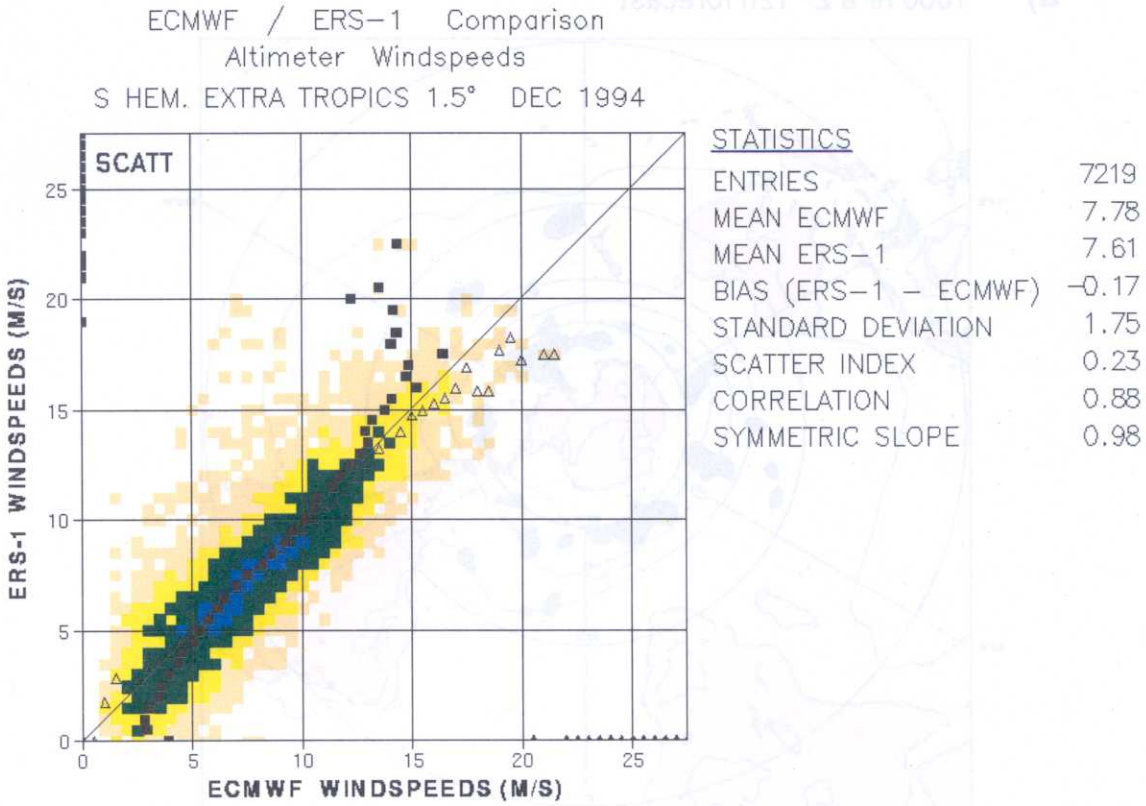

b)

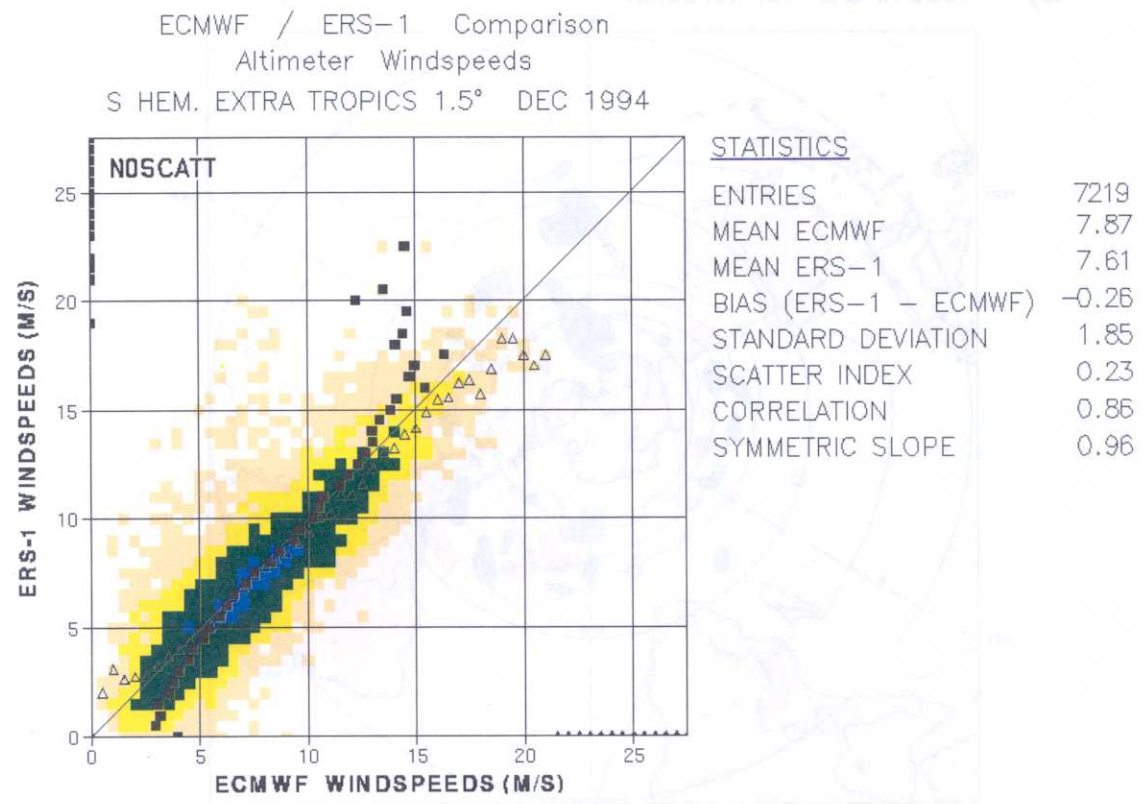

Fig 9: 2-D histogram of first guess and ERS-1 altimeter 10 metre wind speeds for the SCATT (a) and the NOSCATT (b) experiments in the Southern Hemisphere. The colours are a function of the number of data in each wind speed bin. Altimeter wind speeds have been checked and averaged at 1.5° resolution in ECMWF's wave prediction system.

a) 1000 hPa Z* 12h forecast

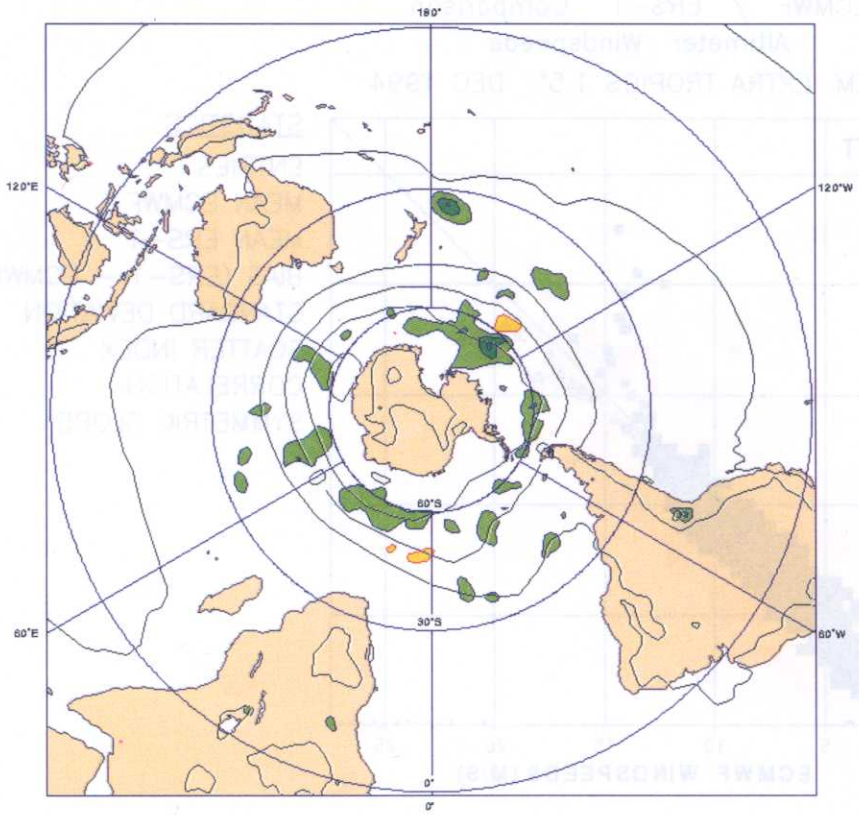

b) 1000 hPa Z* 48h forecast

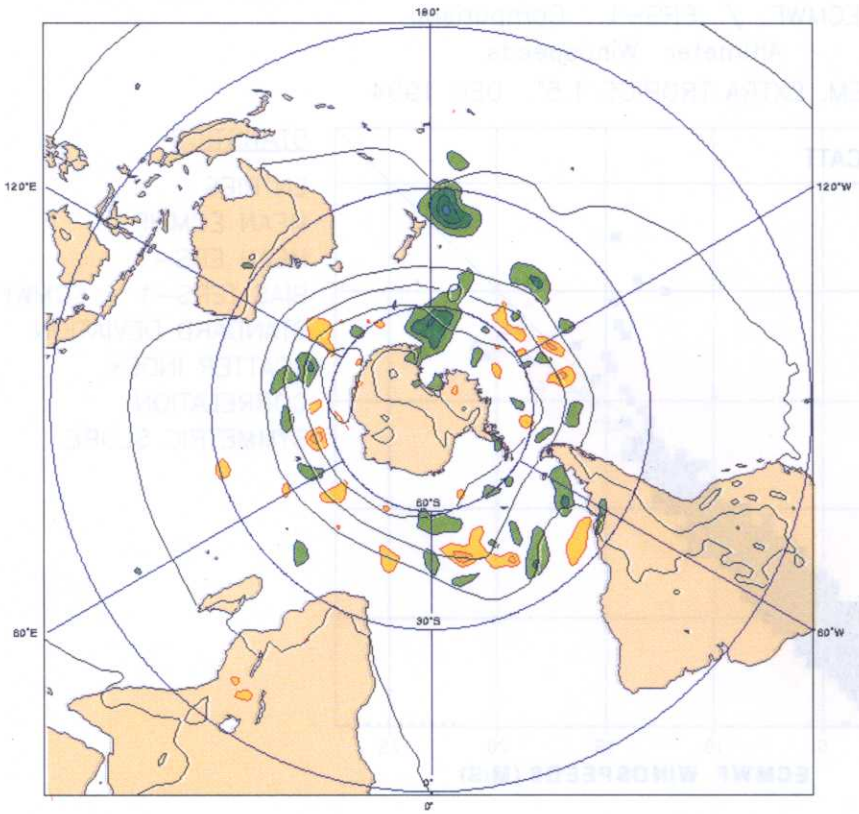

Fig 10: Difference between the SCATT and NOSCATT 12-hour (a)) forecast error RMS for the 1000 hPa geopotential, taking the SCATT analyses as reference. Green and blue colours indicate the areas where the differences are lower than -5 m (SCATT forecasts closer to the analyses), and yellow and red colours differences higher than 5 m. Contour interval is 5 m, and the mean 1000 hPa geopotential is plotted on top (black contour lines).
Fig 10 b) is the same, but for 48-hour forecast.

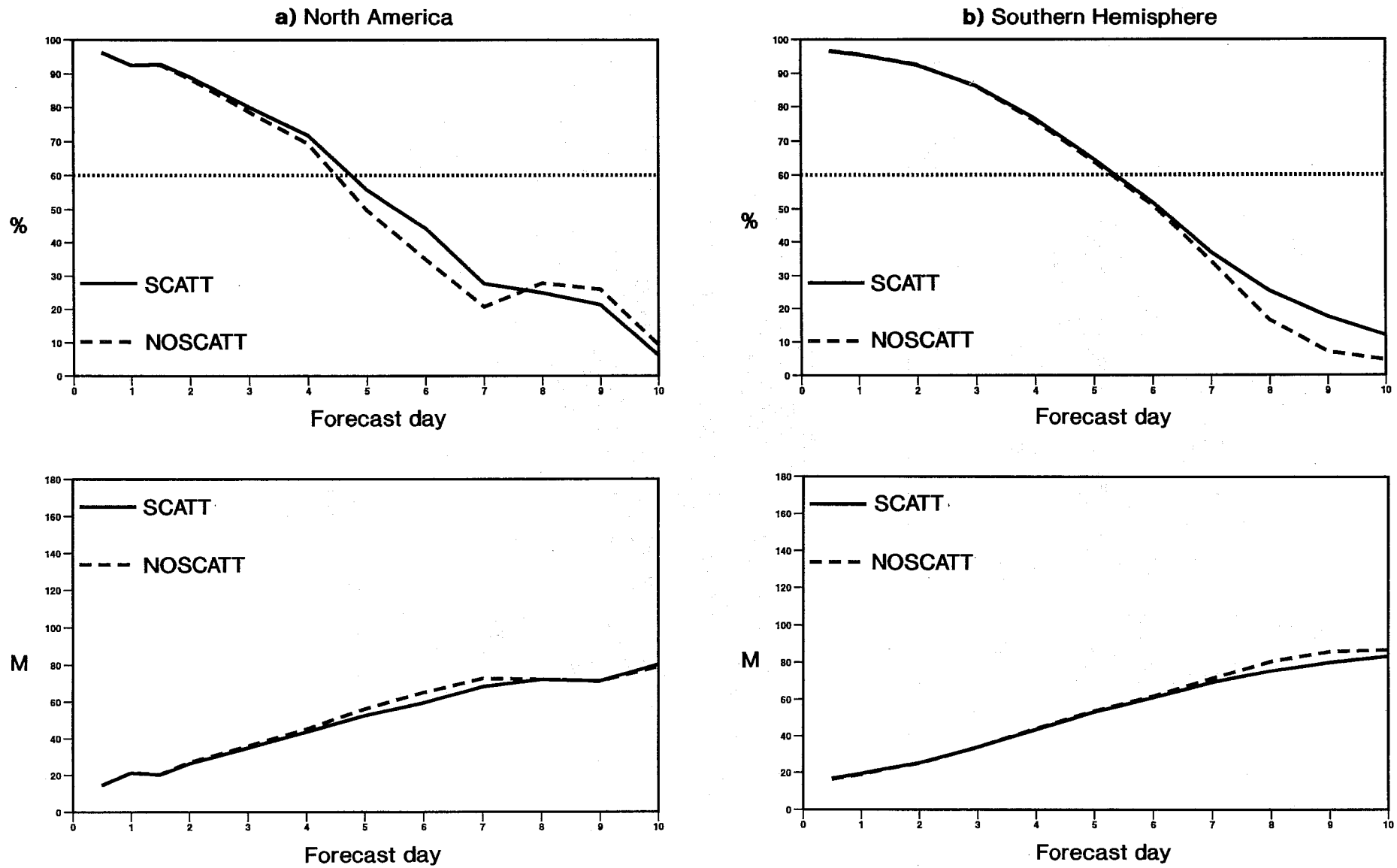

Fig 11: Forecast scores of the SCATT (solid line) and NOSCATT (dashed line) experiments, for Northern America (a) and the Southern Hemisphere (b) . The reference is the ECMWF's operational T213 optimal interpolation analysis, and the scores are computed for the 1000 hPa geopotential in terms of anomaly correlation (upper plot) and RMS error (lower plot), as a function of the forecast range.

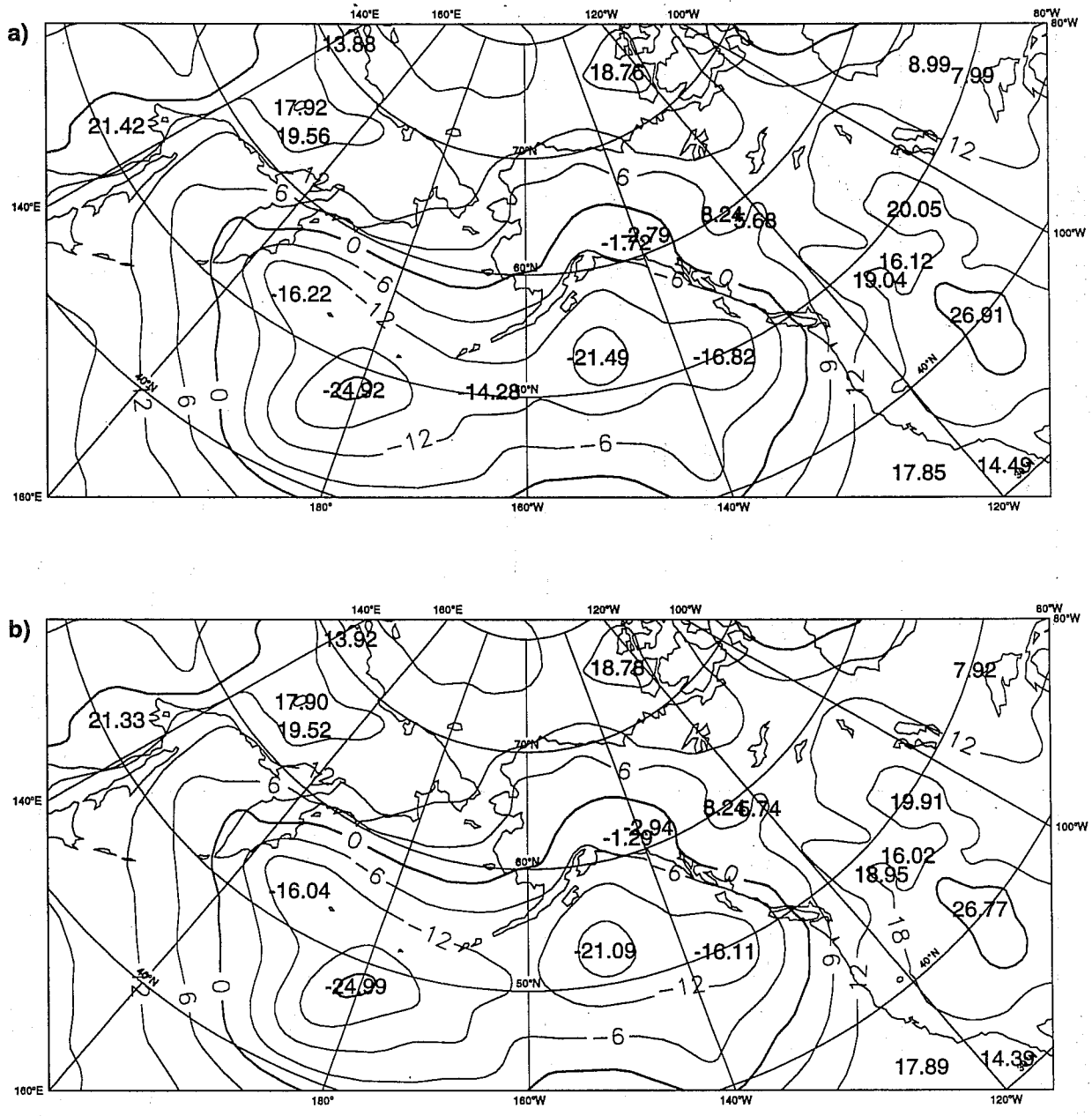

Fig 12: 1000 hPa geopotential analysis on 17 December 1994 at 12 UT over the Northern Pacific for the SCATT (a) and NOSCATT (b) experiments. Contour units are decametres.

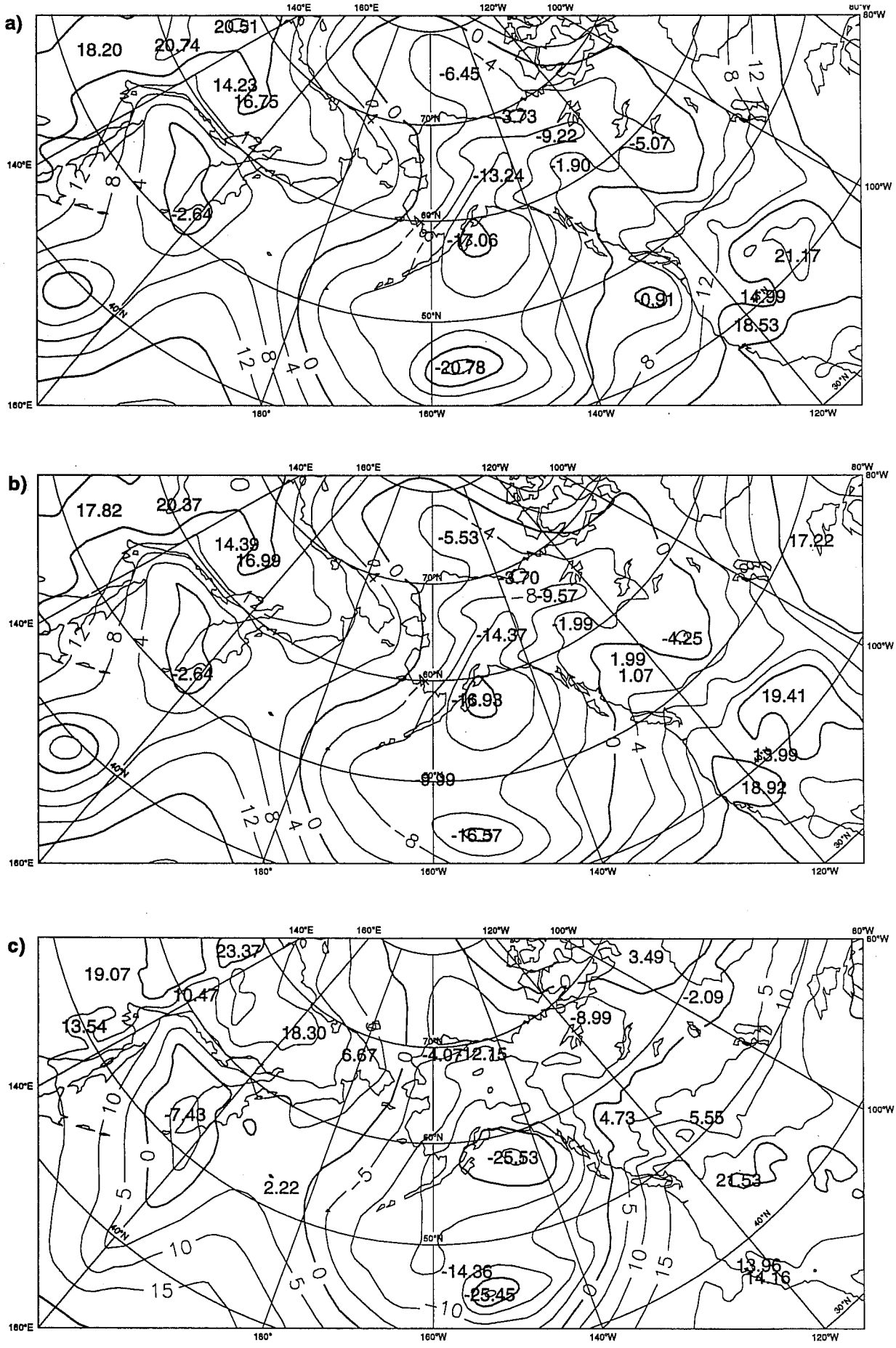

Fig 13: 1000 hPa geopotential 96-hour forecasts initialized from the SCATT (a) and NOSCATT (b) analyses shown in Fig 12. The verifying operational analysis is shown in Fig 13 c).

APPENDIX

The re-tuning of the wind speed dependency of the CMOD4 transfer function has been expressed as a bias correction term which is added to the wind speed retrieved using the original CMOD4 formulation (*Stoffelen and Anderson*, 1995). This bias correction, derived from the comparison between collocated scatterometer and buoy winds (see text), has been fitted by the following third degree polynomial between 2 and 20 m/s, as a function of the original CMOD4 wind speed:

$$V_{SCATT} = V_{CMOD4} + CORR(V_{CMOD4}) \text{ (m/s)} \quad (1)$$

with $CORR(V_{CMOD4}) = a\ V_{CMOD4}^{3} + b\ V_{CMOD4}^{2} + c\ V_{CMOD4} + d$

$a = 2.878\ 10^{-3}$, $b = -8.869\ 10^{-2}$, $c = 9.298\ 10^{-1}$, $d = -2.369$.

The value of the correction is -0.84 m/s for V_{CMOD4} = 2 m/s and 3.77 m/s for V_{CMOD4} = 20 m/s. In an equivalent way, the correction can also be incorporated in the CMOD4 forward model by resolving Equation (1), with V_{CMOD4} being the unknown variable.